ELECTRON IMPACT INDUCED FRAGMENTATION OF 4-ARYL-4,6,7,8-TETRAHYDRO-1*H*,3*H*- QUINAZOLINE-2,5-DIONES

Klaus K. Mayer, * [a] Stefan Dove, * [a] Herwig Pongratz, [a] Mevlüt Ertan, [b] and Wolfgang Wiegrebe [a] #)

[a] Faculty of Chemistry and Pharmacy, University, D-93040 Regensburg / Germany
[b] Faculty of Pharmacy, Hacettepe-University, Ankara / Turkey

Abstract - The molecular ions ($M^{+\bullet}$) of 4-substituted aryl-4,6,7,8-tetrahydro-1*H*,3*H*-quinazoline-2,5-diones (Biginelli compounds) (**2** - **18**) decompose by loss of the substituents X of the phenyl group (X = *o*-F; *o*-, *m*-, *p*-Cl, Br, OCH_3, CH_3; 2,3-, 2,4-, 2,6-, 3,4-dichloro) giving rise to prominent $(M - {}^{\bullet}X)^+$ ions at 70 and 12 eV, respectively. In the cases of *o*-Cl and *o*-Br substitution, the $M^{+\bullet}$ is extremely unstable. In general, metastable $M^{+\bullet}$ (1st ffr) eliminates preferably $H^{\bullet}$, that of **15** (2,6-dichloro), however, exclusively a chlorine atom. As corroborated by ^2H-labelling, reversible H-migration from C-4 to the phenyl group takes place (**1**, **1a** - **1c**). The collisional activation spectra of the $(M - {}^{\bullet}X)^+$ ions of **3** (*o*-Cl) and **6** (*o*-Br) are identical but different from the indistinguishable spectra of the $(M - {}^{\bullet}X)^+$ ions of **4** (*m*-Cl), **5** (*p*-Cl), **9** (*o*-OCH_3), **11** (*p*-OCH_3), and **14** (*p*-CH_3). Semiempirical MO calculations (MOPAC 6.0, PM 3 Hamiltonian) of the $M^{+\bullet}$ of all *ortho*-substituted derivatives support a close interaction of *o*-Cl and *o*-Br with the carbonyl oxygen, leading to elimination of these substituents and affording cyclic oxonium ions. In the other cases loss of $X^{\bullet}$ is explained as a consequence of 4-H migration to the phenyl group.

INTRODUCTION

Derivatives of dihydropyridine-5-carboxylates are of interest as Ca^{2+} antagonists of the nifedipine type.[1] As it was proposed that the calcium-antagonistic activity is associated with the antiperiplanar conformation of the ester group, annelated tetrahydropyrimidine derivatives such as 4-aryl-4,6,7,8-tetrahydro-1*H*,3*H*-quinazoline-2,5-diones and their thio analogues were synthesized and tested for calcium antagonistic effects.[3]

Since information on electron impact induced fragmentations of tetrahydropyrimidine-2,5-diones is rather scarce[4] we report here on a systematic MS study on the title compounds (**1** - **18**). Additionally, semiempirical quantum chemical and molecular mechanics calculations were applied to support the interpretation of some of the results.

#) Dedicated with warm regards to Prof. Dr. Narao Takao, Kobe Pharmaceutical University, Japan, on the occasion of his 70th birthday.

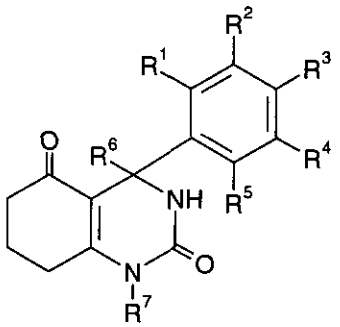

	R^1	R^2	R^3	R^4	R^5	R^6	R^7
1	H	H	H	H	H	H	H
2	F	H	H	H	H	H	H
3	Cl	H	H	H	H	H	H
4	H	Cl	H	H	H	H	H
5	H	H	Cl	H	H	H	H
6	Br	H	H	H	H	H	H
7	H	Br	H	H	H	H	H
8	H	H	Br	H	H	H	H
9	OCH_3	H	H	H	H	H	H
10	H	OCH_3	H	H	H	H	H
11	H	H	OCH_3	H	H	H	H
12	CH_3	H	H	H	H	H	H
13	H	CH_3	H	H	H	H	H
14	H	H	CH_3	H	H	H	H
15	Cl	H	H	H	Cl	H	H
16	Cl	Cl	H	H	H	H	H
17	Cl	H	Cl	H	H	H	H
18	H	Cl	Cl	H	H	H	H
19	Cl	H	H	H	H	H	CH_3
1a	H	H	H	H	H	D	H
1b	D	D	D	D	D	H	H
1c	D	D	D	D	D	D	H

RESULTS AND DISCUSSION

MS of compounds (**1 - 18**)

The EI MS spectrum (70 eV) of 4-phenyl-4,6,7,8-tetrahydro-1*H*,3*H*-quinazoline-2,5-dione (**1**) is characterized by an abundant molecular ion peak and by the presence of only a few significant fragment ions (HR-MS) at m/z 241 [(M - H$^\bullet$)$^+$; 34%]; m/z 225 [(M - $^\bullet$OH)$^+$; 2%]; m/z 198 [(241 - HNCO)$^{+\bullet}$; 3%], m/z 186 [(M - C_3H_4O)$^{+\bullet}$; 10%], m/z 165 [(M - $^\bullet C_6H_5$)$^+$; 100%], and m/z 55 ($C_3H_3O^+$; 5%). Low-energy $M^{+\bullet}$ (12 eV) gives rise to the base peak and decomposes by loss of H$^\bullet$ (1%), C_3H_4O (1%) or $^\bullet C_6H_5$ (5%). Metastable molecular ions (1st field free region; 1st ffr) lose mainly H$^\bullet$ (100%) and to a minor extent C_3H_4O (1%) and $^\bullet C_6H_5$ (2%). D-Labelling in compounds (**1a - 1c**) revealed, that the H-atoms which are

eliminated from $M^{+\bullet}$ arise from various positions (Table 1). High-energy $M^{+\bullet}$ emits preferably D-atoms from C-4 and the C_6D_5-group whereas in the case of metastable $M^{+\bullet}$ predominant loss of $H^{\bullet}$ takes place.

Table 1. Loss of $H^{\bullet}$ vs $D^{\bullet}$ from $M^{+\bullet}$ (70/12 eV) and metastable $M^{+\bullet}$ (1st ffr) of **1a-1c** (%).

compd	70 eV		12 eV		1st ffr	
	Δ H	Δ D	Δ H	Δ D	Δ H	Δ D
1a	60	40	90	10	98	2
1b	50	50	85	15	92	8
1c	35	65	80	20	97	3

Moreover, there is evidence from the data in Table 1 (**1c**) that these H-atoms are originally part of the unlabelled cyclohexenone increment of **1**. In addition, it could be deduced from the spectra of **1a** - **1c** that a reversible exchange of 4-H and the aromatic H-atoms occurs before $^{\bullet}C_6H_5$-elimination takes place (Table 2). $M^{+\bullet}$ of **1a** loses $^{\bullet}C_6H_5$ and $^{\bullet}C_6H_4D$, $M^{+\bullet}$ of **1b** $^{\bullet}C_6HD_4$ and $^{\bullet}C_6D_5$, whereas $M^{+\bullet}$ of **1c** ejects exclusively $^{\bullet}C_6D_5$ radicals.

Table 2. Loss of phenyl radicals from **1a** , **1b** (%).

condition	**1a**		**1b**	
	$(M - {}^{\bullet}C_6H_5)^+$	$(M - {}^{\bullet}C_6H_4D)^+$	$(M - {}^{\bullet}C_6HD_4)^+$	$(M - {}^{\bullet}C_6D_5)^+$
70 eV	85	15	18	82
12 eV	82	18	25	75
1st ffr	21	79	76	24

Comparable hydrogen exchange reactions preceding decomposition of radical cations are well established to proceed by [1,2] or [1,3] H shifts, *e.g.* in the case of tetralin,[5] 1-phenyltetralin[6] and toluene.[7] Analogously the interchange of $H^{\bullet}$ located at C-4 and the phenyl groups can be explained (Figure 1).

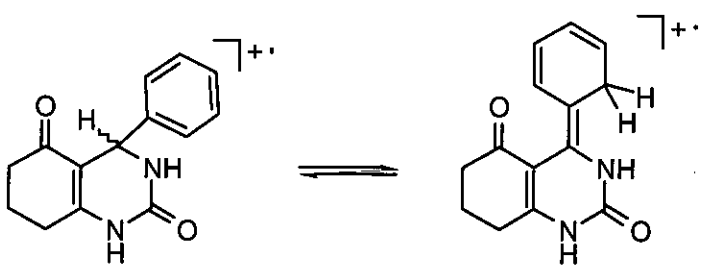

1 **1´**

Figure 1

Introduction of substituents X at the phenyl group affords additional strong fragment ions in the 70 eV spectra of **2** - **14** (Table 3). The respective $M^{+\bullet}$ loses the substituents Cl, Br, or OCH_3 preferentially from the *ortho*-position, but also loss of *meta*- as well as *para*-X takes place giving rise to ions of large intensities. In the case of **2** elimination of *o*-F is suppressed by ejection of HF and the consecutive loss of $H^{\bullet}$ from the resulting $(M - HF)^{+\bullet}$ ion. In particular, *o*-Cl (**3**) and *o*-Br (**6**) substituents cause a drastic change in the fragmentation pattern; the $M^{+\bullet}$ is obviously extremely unstable (< 0.1% rel. int.; 70 and 12

eV) and decomposes predominantly to $(M - {}^{\bullet}X)^+$ ions. Competing fragmentations as losses of H$^{\bullet}$ or ${}^{\bullet}C_6H_4X$ are of minor importance, especially at low ionization energies. $(M - {}^{\bullet}X)^+$ ions of the other compounds (**2**, **4**, **5**, **7** - **14**), however, undergo a strong decrease of intensities at 12 eV, and the respective $M^{+\bullet}$ affords the base peak. All $(M - {}^{\bullet}X)^+$ ions are capable of eliminating HNCO (HR-MS) at 70 eV, but only those derived from **3** and **6** produce intensive $[(M - {}^{\bullet}X) - HNCO]^+$ ions at 70 and 12 eV.

Table 3. Principal ions in the MS (70/12 eV) of compounds (**2-14**) (% rel. int.; sum of $^{35/37}Cl$ / $^{79/81}Br$).

compd	$M^{+\bullet}$	$(M - H^{\bullet})^+$	$(M - X^{\bullet})^+$	$[M - (CO+C_2H_4)]^{+\bullet}$	$(M - {}^{\bullet}C_6H_4X)^+$	$[M - (X^{\bullet}+HNCO)]^+$
2[*)]	61/100	16/1	3/0.2	19/1	100/1	4/0.3
3	<0.1/<0.1	1/0.1	100/100	4/1	33/2	37/11
4	55/100	12/2	44/15	6/1	100/10	0.2/-
5	82/100	35/2	49/12	10/1	100/11	0.3/-
6	<0.1/<0.1	1/0.1	100/100	6/-	38/1	66/8
7	62/100	15/1	60/9	9/-	100/7	3/-
8	65/100	17/2	57/9	11/1	100/6	3/-
9	66/100	20/2	100/25	2/2	63/2	5/-
10	59/100	20/2	38/6	13/1	100/6	1/-
11	100/100	50/3	79/10	28/2	85/2	2/-
12	23/100	16/12	34/11	7/1	100/15	2/-
13	60/100	21/2	32/5	9/1	100/7	2/-
14	78/100	33/3	54/6	3/1	100/5	2/-

*) **2** : $(M - HF)^{+\bullet}$ 14/7; $[M - (HF+H^{\bullet})]^+$ 98/33.

The dichloro substituted compounds (**15** - **18**) follow the same fragmentation pathways as their monochloro analogues (Table 4).

Table 4. Principal ions in the MS (70/12 eV) of compounds (**15-18**) (% rel. int.; sum of $^{35/37}Cl$).

compd	$M^{+\bullet}$	$(M - H^{\bullet})^+$	$(M - Cl^{\bullet})^+$	$[M - (CO+C_2H_4)]^{+\bullet}$	$[M - (Cl^{\bullet}+HCl)]^+$	$[M - (Cl^{\bullet}+HNCO)]^+$	$(M - {}^{\bullet}C_6H_3Cl_2)^+$
15	3/6	0.1/-	100/100	11/1	46/2	72/8	47/1
16	<0.1/<0.1	0.5/0.1	100/100	6/-	-	42/8	40/1
17	1/1	0.5/-	100/100	9/-	1/-	48/6	33/2
18	60/100	11/2	85/35	8/1	-	14/2	100/11

The $M^{+\bullet}$ of **15** - **17** (*o*-Cl) is very unstable and decomposes rapidly in the ion source to strong $(M - {}^{\bullet}Cl)^+$ ions which release preferentially HNCO. Only in the case of the dichloro compound (**15**), the $(M - {}^{\bullet}Cl)^+$ ion additionally loses HCl to a remarkable extent. Metastable $M^{+\bullet}$ decomposing in the 1st ffr (B/E scan; 70 / 12 eV) (**4**, **5**, **7** - **14**, **17**, **18**) loses predominantly H$^{\bullet}$ and only minor quantities of ${}^{\bullet}X$ (Table 5); in sharp contrast to this, metastable $M^{+\bullet}$ of **15** eliminates exclusively (99 / 100%) one of the *o*-${}^{\bullet}Cl$ atoms and thereupon HCl. Metastable $M^{+\bullet}$ of **2** gives rise to strong $(M - HF)^{+\bullet}$ - and $[(M - HF) - {}^{\bullet}H]^+$ ions (72 / 85 and 28 / 15 %, respectively).

The 1-methyl analogue (**19**) of the *o*-chloro compound (**3**) forms a slightly more stable $M^{+\bullet}$ [0.7 / 0.2 % rel. int. at 70 / 12 eV; $(M - {}^{\bullet}Cl)^+$: 100 / 100 %]. $M^{+\bullet}$ of **19** loses preferably H$^{\bullet}$ (96 % Σ) and ${}^{\bullet}Cl$ (4 % Σ) in accord with the majority of compounds in Table 5.

Table 5. Loss of H$^{\bullet}$ vs. X$^{\bullet}$ from metastable M$^{+\bullet}$ of compounds (**4, 5, 7-15, 17, 18**) (1st ffr; B/E scan; 70/12 eV; [%])

compd	**4**	**5**	**7**	**8**	**9**	**10**	**11**	**12**	**13**	**14**	**15**	**17**	**18**
$(M-H^{\bullet})^+$													
70 eV	98	98	94	96	94	94	95	90	98	98	1	97	96
12 eV	99	99	96	98	98	97	98	95	99	99	-	98	98
$(M-X^{\bullet})^+$													
70 eV	2	2	6	4	6	6	5	10	2	2	99	3	4
12 eV	1	1	4	2	2	3	2	5	1	1	100	2	2

The present results confirm that formation of (M - $^{\bullet}$X)$^+$ ions is one of the most favourable reactions of high energy molecular ions of the title compounds in the ion source (70 eV); at low ionization energies (12 eV) they give rise to the predominant fragment ions. Similarily, metastable molecular ions emit the *o*-, *m*-, and *p*-substituents, elimination of H$^{\bullet}$, however, prevails over loss of X$^{\bullet}$.

The data derived from the spectra of **1** and its deuteromers (**1a - 1c**) (Tables 1 and 2) evidence that the H-atoms, lost from metastable M$^{+\bullet}$, arise mainly from C-4 and the phenyl group at 70 eV, but preferably from other positions at 12 eV. Metastable M$^{+\bullet}$ loses even 92 - 98 % H$^{\bullet}$ and only 2 - 8 % D$^{\bullet}$. Furthermore, hydrogen exchange between C-4 and the phenyl group takes place (losses of $^{\bullet}C_6H_4D$ and $^{\bullet}C_6HD_4$, respectively) and possibly preceeds elimination of $^{\bullet}$X, too.

A priori several mechanisms can explain the generation of (M - $^{\bullet}$X)$^+$ ions and, correspondingly, different structures of these ions:

1) A simple bond cleavage in the M$^{+\bullet}$ without any assistance by a neighbouring group would form phenyl cations in which the positive charge is mainly located at the *ortho*-, *meta*-, or *para*-position. Direct loss of X$^{\bullet}$ from an aromatic ring is a high energy process, especially in the cases of X = F (5.4 eV), H (4.8 eV), CH_3 (4.3 eV), and OCH_3 (4.2 eV).[8] This can be ruled out at least for the obviously easy elimination of Cl (3.6 eV) and Br (3.1 eV) from the *o*-positions of **3**, **6**, and **15 - 17**.

2) (M - $^{\bullet}$X)$^+$ ions arise from an intramolecular displacement of the *ortho* substituents (ortho-effect[9]) by the neighbouring carbonyl group at C-5 affording cyclic oxonium ions. In the cases of benzalacetones,[10] cinnamic acids,[11] or 2-benzylidenecyclohexanones[12] the pertinent M$^{+\bullet}$ loses the substituents (X = Hal, OCH_3, CH_3, NO_2) from all positions of the phenyl group in the order *o*- >> *m*- > *-p*; the ejection of *m*- and *p*-substituents is preceeded by 1,2-H shifts around the aromatic nucleus after ring closure.[13] This mechanism seems to be valid only, if a 3-aryl prop-2-enone skeleton is part of a molecule. As this is not the case in compounds (**1 - 19**), the application of this concept is only possible if it is assumed, that **1** isomerizes by a 1.3 H shift to **1´´** (Figure 2). There is, however, no direct evidence for this reaction.

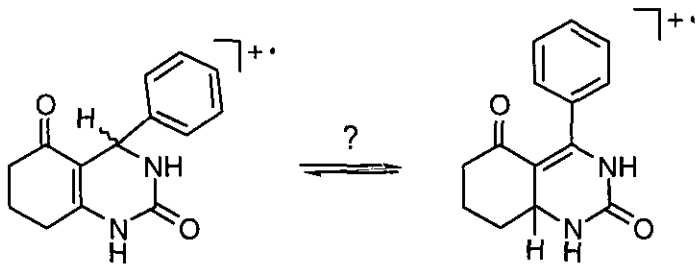

1 **1´´**

Figure 2

4-H migration into the phenyl group, on the other hand, is proved to occur in high and low energy $M^{+\bullet}$ (Table 2). Therefore, it is conceivable that in the cases of all substituents X, except *o*-Cl and *o*-Br, at least a part of the population of $(M - {}^{\bullet}X)^+$ ions arises from isomerized $M^{+\bullet}$ (Figure 1) with tetracoordinated C-atoms in the *o*-, *m*-, and *p*-position of the phenyl ring, which eventually decompose.

Information on the structure of $(M - {}^{\bullet}X)^+$ ions is provided by their decomposition. Unstable $(M - {}^{\bullet}X)^+$ ions of **3**, **6**, and **15 - 17** give rise to large signals at m/z 141 $[(M - {}^{\bullet}X) - HNCO]^+$ at 70 eV which decrease sharply at 12 eV (Tables 3 and 4). In the 70 and 12 eV spectra of the rest of the compounds, the respective signals are small or absent. Metastable $(M - {}^{\bullet}X)^+$ ion of **1 - 14** loses predominantly $H^{\bullet}$ (93 - 98 %) or small amounts of HNCO, the latter losses increase distinctly in the cases of the dichlorophenyl compounds (**15 - 17**) (Table 6). A slight alteration in favour of HNCO elimination is already noticeable for **3** (*o*-Cl) and **6** (*o*-Br), which may be due to different amounts of internal energies in the $(M - {}^{\bullet}X)^+$ ions. The collisional activation (CA)[14] spectra of **3**, **6**, and **4**, **5**, **9**, **11**, **14**, obtained by CA with He in the 1st ffr (Table 7), show more clearly that $(M - o\text{-}Cl^{\bullet} / o\text{-}Br^{\bullet})^+$ ions differ from $(M - m / p\text{-}Cl; o- / p\text{-}OCH_3; p\text{-}CH_3)^+$ ions. Consequently, these two groups of isomeric ions have different structures, possibly **a** and **b** (Figure 3) (or a different mixture of non-interconverting structures), whereas the CA spectra within each group are virtually indistinguishable.

Table 6. MS of metastable $(M - X^{\bullet})^+$ ions (70eV, B/E scan, 1st ffr; % sum of fragment ions)

compd	Δ H	Δ HNCO	Δ Cl	Δ HCl
1	97.6	2.4	-	-
3	94.3	5.7	-	-
4, 5	98.0	2.0	-	-
6	93.4	6.6	-	-
7, 8	97.1	2.9	-	-
9 -11	98.0	2.0	-	-
12	96.2	3.8	-	-
13, 14	97.8	2.2	-	-
15	0.6	27.5	9.4	62.5
16	64.5	33.5	1.0	1.0
17	74.5	23.9	0.7	0.9
18	96.1	2.3	0.7	0.9

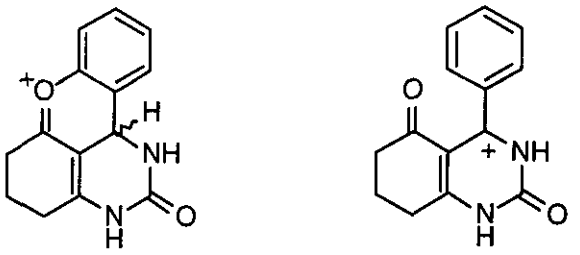

Figure 3

Table 7. CA spectra of $(M - X^{\cdot})^{+}$ ions (m/z 241) (* ion intensities were not used for normalization)

m/z	**3** *o*-Cl	**6** *o*-Br	**4** *m*-Cl	**5** *p*-Cl	**9** *o*-OMe	**11** *p*-OMe	**14** *p*-Me
51	0.4	0.4	0.6	0.7	0.4	0.4	0.5
55	0.8	0.7	1.9	1.7	1.8	1.6	1.7
76	0.5	0.6	0.7	0.7	0.8	0.6	0.6
77	1.4	1.3	3.2	2.8	3.1	3.0	2.9
89	0.6	0.6	1.0	1.1	0.9	1.0	1.0
102	0.7	0.8	0.9	0.9	1.0	0.8	1.0
103	0.5	0.4	0.9	0.9	0.9	0.8	0.8
104	2.3	2.1	5.6	6.0	5.8	6.0	5.7
105	0.3	0.3	0.8	0.8	0.8	0.7	0.9
114	0.6	0.6	0.8	0.7	0.8	0.6	0.8
115	2.1	2.3	2.7	2.8	2.6	2.9	2.7
116	0.6	0.7	1.1	1.0	0.9	0.8	1.0
120	1.4	1.2	1.0	0.8	0.9	1.0	0.8
127	1.3	1.2	2.2	2.1	2.1	2.2	2.0
128	1.4	1.4	2.1	2.1	2.2	2.3	2.1
140	0.9	1.2	1.0	1.2	1.2	1.0	1.1
141	0.6	0.7	0.8	0.6	0.8	0.7	0.9
142	0.6	0.6	0.9	1.0	0.8	0.8	1.0
143	0.7	0.6	1.1	1.3	1.2	1.0	1.2
153	0.7	0.6	0.9	0.8	0.7	0.7	0.9
154	0.5	0.5	0.8	0.9	0.9	0.9	0.7
155	1.0	0.9	1.9	1.8	1.9	1.9	1.8
156	1.2	1.1	1.6	1.7	1.5	1.8	1.6
162	0.4	0.4	0.7	0.8	0.8	0.7	0.9
163	2.0	2.2	3.1	3.2	2.8	3.0	3.0
165	2.0	2.1	2.1	2.0	1.9	2.0	2.1
167	0.8	0.9	1.1	1.3	1.3	1.2	1.2
168	1.2	1.2	1.3	1.4	1.4	1.3	1.4
169	2.1	2.3	0.9	1.1	1.0	1.1	1.0
170	2.4	2.5	1.9	2.0	1.8	2.2	1.9
171	0.7	0.7	1.1	1.0	1.0	0.9	0.9
180	0.5	0.4	0.6	0.7	0.7	0.6	0.6
181	1.1	1.0	0.7	0.6	0.7	0.7	0.8
182	2.0	2.0	1.9	2.0	2.0	1.9	2.1
183	1.0	1.0	1.0	1.1	1.1	1.2	1.0
184	4.3	4.0	6.1	6.2	5.9	6.3	6.2
185	1.1	1.0	2.1	2.1	1.9	2.0	2.1
186	0.9	0.9	2.5	2.7	2.6	2.5	2.7
194	0.3	0.3	0.4	0.4	0.6	0.4	0.5
195	0.7	0.6	0.7	0.8	0.9	0.7	0.9
196	7.5	7.8	1.7	1.7	1.6	1.5	1.5
197	15.1	15.6	1.7	1.6	1.9	1.6	1.8
198*	(119.4)	(157.7)	(5.0)	(4.8)	(4.9)	(3.9)	(4.5)
199	14.1	14.5	1.6	1.6	1.4	1.3	1.6
209	0.4	0.4	1.7	1.6	1.6	1.7	1.5
210	0.4	0.4	0.4	0.6	0.5	0.5	0.7
211	3.4	3.5	9.4	9.3	9.5	9.6	9.3
212	4.1	4.3	3.4	3.4	3.6	3.5	3.6
213	2.6	2.9	3.3	3.6	3.5	3.3	3.4
223	3.1	2.7	5.8	5.9	6.0	6.1	6.0
224	1.0	0.7	1.6	1.7	1.7	1.5	1.7
225	0.5	0.5	1.0	0.9	1.0	1.3	1.0
237	1.7	2.0	3.4	3.6	3.4	3.3	3.5
238	0.9	0.8	1.9	1.6	1.7	1.9	1.8
239*	(21.7)	(21.4)	(23.4)	(24.0)	(69.5)	(58.6)	(54.3)
240*	(68.0)	(59.8)	(48.2)	(54.1)	(180.1)	(71.0)	(165.2)

Theoretical calculations

Since product ion structures arising from *o*-Cl and *o*-Br substituted molecular ions cannot be regarded as established unequivocally, only plausible but rather speculative mechanisms could be advanced. As elimination of X$^{\bullet}$ is reduced with substituents in *meta* and in *para* positions which cannot approach the carbonyl oxygen O5, *e.g.*, for favourable cyclization, the mechanism in question must include a direct intramolecular interaction which depends on steric constraints and which is not energetically demanding, since the reaction is predominant at low ionization energies (12 eV), too.

To suggest what might happen, semiempirical quantum chemical (QCPE program MOPAC 6.0, PM3 Hamiltonian) and molecular mechanics calculations (Tripos force field, software SYBYL 6.3, Tripos Ass.) have been performed on a Silicon Graphics Indigo^2 Solid Impact workstation, considering all *ortho*-substituted derivatives. For numbering of atoms, see Figure 4:

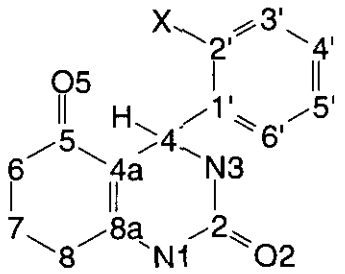

Figure 4

The strategy was as follows:

1) Investigation of the minimum energy conformers of the molecular ion, using MOPAC with the unrestricted Hartree-Fock method to save computing time.

2) Calculation of the potential function of the phenyl ring rotation around the C4-C1' bond (torsion angle N3-C4-C1'-C2' as reference). Molecular mechanics with the Tripos force field and the SYBYL Gridsearch routine (minimization of each degree of freedom except the reaction coordinate) was used in this case since generally rotational barriers are not well reflected by semiempirical methods. To approximate the electronic structure of the molecular ions, the MOPAC charges were applied to the Coulomb potential.

3) Refined semiempirical calculations of the molecular ions in their energy minimum conformations and in conformations representing possible "transition states" (see below). The restricted Hartree-Fock method with configuration interaction including four MOs (the original LUMO and SOMO as well as the next two lower MOs) was used.

4) Estimation of reaction enthalpies from DHF = HF (M - X$^{\bullet}$)$^+$ + HF (X$^{\bullet}$) - HF (M$^{\bullet+}$).

The calculation of molecular ions by semiempirical methods is of course by far not exact, and even *ab initio* approaches with low- and medium-sized basis sets cannot predict small differences of the reactivity. Interpretations are therefore restricted to large, qualitative differences between derivatives parallel to experimental findings.

Results of the theoretical calculations are as follows: Using MOPAC with the eigenvector following gradient routine, all eight molecular ions adopt their global energy minimum conformation at similar values of the torsion angle N3-C4-C1'-C2' between *ca.* 265° and 295° (Table 8). As Figure 5 exemplarily shows for the *o*-Cl derivative, this corresponds to a position of the *ortho* substituents close to the C4a-C8a π-bond, indicating that van der Waals attraction and possibly charge-transfer interactions are responsible for decreasing conformational energy. Apart from C7, the bicyclic system is nearly planar

with an envelope geometry of the cyclohexenone moiety as expected. Of course, inversion of C7 is possible but leads to higher rotational barriers of the phenyl ring due to steric hindrance.

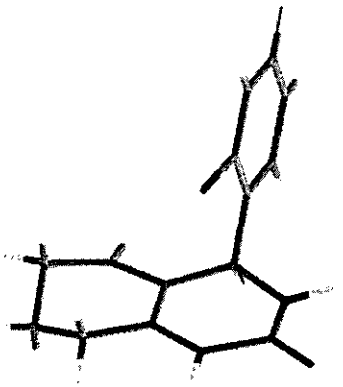

Figure 5. Energy minimum conformation of the *o*-Cl derivative

Molecular mechanics calculations with the Tripos force field principally confirm these results from MOPAC, as indicated by the potential function of the torsion angle N3-C4-C1'-C2' (Figure 6a, energies relative to the absolute minima given). The global minimum of each derivative is near 300°. Only in the case of *o*-CH_3, a second minimum at 115° is almost equal in energy to the first one. In all other cases, this second minimum is 1 to 3 kcal higher. There are two rotational barriers at 0 - 30° and at 180 - 210°, respectively. The latter is always higher, except for *o*-CH_3. Even in the cases of *o*-Br (**6**) and *o,o'*-di-Cl (**15**), this barrier is < 11 kcal/mol. Thus, the energetical conditions even at 12 eV allow rotation of the phenyl ring of each derivative, and the different fragmentation of the molecular ions cannot be due to steric hindrance. With this important information in hand, more precise conformational analyses are not reasonable. It should, however, be noted that rotational barriers of the molecular ions calculated by MOPAC approximately correspond to those from molecular mechanics: examples are *o*-Cl (8.9 kcal/mol), *o*-F (5.6), *o*-Br (9.2), *o*-CH_3 (8.1), and *o*-OCH_3 (6.2).
In conclusion, the ortho substituents may approach the C4a-C8a π-bond in conformations near the energy minimum. If the substituents were split off in this position, the cyclization between O5 and C2' would be a subsequent process. Alternatively, a close approach of O5 and the substituent atom X may be suggested, leading to a nearly simultaneous mechanism of cleavage (elimination) and cyclization (addition). Figure 6b shows the distance O5-X as function of the torsion angle N3-C4-C1'-C2'. In all derivatives, the closest distance below 3 Å occurs at 150-165°, corresponding to energies of 5-9 kcal above the global minimum. To investigate which mechanism is more likely, both alternatives must be considered in calculating electronic structures of the molecular ions by semiempirical methods.

In Table 8, results of the MOPAC calculations of the energy minimum conformers and of the postulated "*transition states*" at *torsion angles* N3-C4-C1'-C2' of about 165° are presented (these states are not transition states along a continuous reaction pathway, but reflect instable states undergoing further transformations not based on the reaction coordinate N3-C4-C1'-C2'). MO energies, AO coefficients (not shown for volume reasons), spin densities, and net atomic charges are the suggested main driving forces for reactivity. As Table 8 indicates, there is, however, no significant and qualitative difference between the electronic structures of the eight energy minimum conformers.

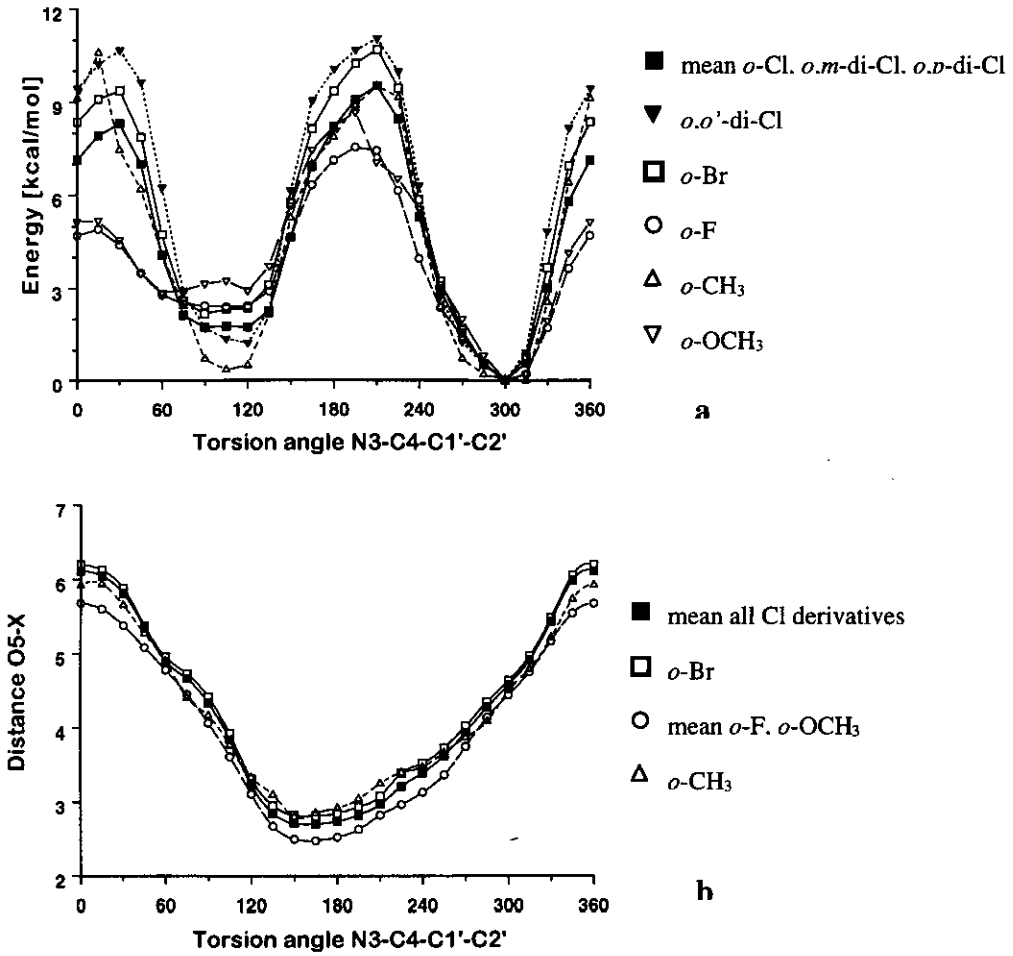

Figure 6. Relative energy **[a]** and distance O5-X **[b]** as function of the torsion angle N3-C4-C1'-C2'.

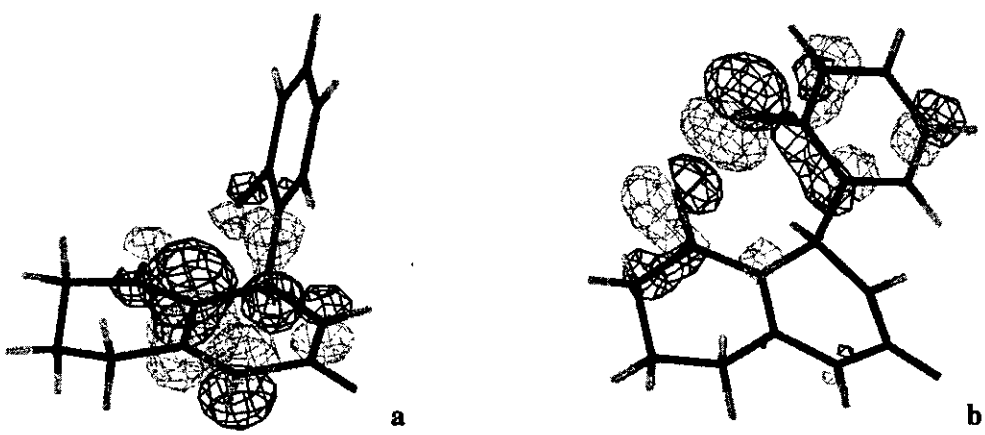

Figure 7. SOMO of the energy minimum conformer **[a]** and the "transition state" **[b]**, *o*-Cl derivative (**3**).

Table 8. Results of MOPAC calculations comparing the energy minimum conformers (M) and postulated "transition states" (T) of the *o*-substituted molecular ions. Abbreviations in the first column are: HF - heat of formation [kcal/mol], E - MO energy [eV], sd - spin density, q - atomic net charge, τ - torsion angle N3-C4-C1'-C2'. Additionally, HF-G of the unionized ground states is given.

	o-Cl	*o,m*-Cl_2	*o,p*-Cl_2	*o,o'*-Cl_2	*o*-Br	*o*-F	*o*-Me	*o*-OMe
HF - G	-48.385	-53.781	-54.725	-52.720	-33.482	-86.835	-50.559	-80.000
HF-M	143.960	139.674	138.864	139.940	155.187	104.854	141.344	107.815
on τ	285.70°	285.88°	286.58°	275.79°	262.06°	293.55°	283.64°	295.06°
HF - T	148.571	144.528	144.048	146.294	165.572	109.634	143.497	113.386
E(SOMO)-G	-10.884	-10.834	-10.847	-10.776	-10.647	-10.908	-10.848	-10.662
E(SOMO)-T	-9.467	-9.465	-9.507	-9.502	-9.516	-10.988	-10.776	-10.653
E(SOMO-1)-G	-12.999	-12.518	-12.503	-12.748	-13.453	-13.291	-12.916	-12.689
E(SOMO-1)-T	-12.898	-12.873	-12.708	-12.835	-13.024	-13.249	-13.027	-12.681
E(SOMO-2)-G	-13.435	-13.315	-13.206	-13.369	-13.532	-13.555	-13.176	-13.332
E(SOMO-2)-T	-13.457	-13.096	-12.929	-13.035	-13.351	-13.581	-13.450	-13.516
sd(C4a) - G	0.6058	0.5450	0.5751	0.5778	-0.6045	-0.5942	-0.6024	-0.5736
sd(C4a) - T	-0.1749	0.1712	0.1823	0.1654	-0.1661	-0.6058	-0.5458	-0.5658
sd(C8a) - G	0.2935	0.2636	0.2618	0.2871	-0.2991	-0.2786	-0.3096	-0.2774
sd(C8a) - T	-0.0551	0.0557	0.0585	0.0432	-0.0884	-0.3066	-0.2496	-0.2931
sd(O5) - G	-0.3416	-0.3066	-0.3066	-0.3229	0.3356	0.3424	0.3359	0.3248
sd(O5) - T	0.5400	-0.5718	-0.5665	-0.5594	0.7467	0.3688	0.3383	0.3282
sd(C2') - G	-0.0165	-0.0201	0.0022	-0.0232	-0.0018	-0.0172	0.0378	-0.0184
sd(C2') - T	-0.1452	0.1551	0.1364	0.1066	-0.0644	-0.0475	-0.1927	-0.1179
sd(X) - G	0.1740	0.1579	0.1307	0.2386	-0.2932	-0.0279	-0.0885	-0.0140
sd(X) - T	1.1658	-1.1494	-1.1656	-1.0368	1.0668	0.0064	0.1096	0.0722
q(C4a) - G	-0.0672	-0.1031	-0.0944	-0.0916	-0.0739	-0.0562	-0.0660	-0.0665
q(C4a) - T	-0.4064	-0.4152	-0.4083	-0.4159	-0.3929	-0.0382	-0.0980	-0.0813
q(C8a) - G	-0.0377	-0.0318	-0.0306	-0.0317	-0.0327	-0.0370	-0.0456	-0.0347
q(C8a) - T	0.0952	0.0946	0.0955	0.1015	0.1019	-0.0440	-0.0285	-0.0379
q(O5) - G	-0.2212	-0.2314	-0.2294	-0.2243	-0.2188	-0.2219	-0.2167	-0.2286
q(O5) - T	-0.4370	-0.4437	-0.4374	-0.4379	-0.3709	-0.1950	-0.2322	-0.2162
q(C2') - G	-0.1087	-0.1309	-0.0910	-0.1103	-0.0993	0.0666	-0.0515	0.1292
q(C2') - T	-0.4394	-0.4499	-0.4245	-0.4267	-0.3013	0.0929	-0.0064	0.1378
q(X) - G	0.0590	0.1042	0.0669	0.0905	0.0442	-0.1067	-0.0750	-0.2443
q(X) - T	0.8570	0.8771	0.8603	0.8536	0.6411	-0.0799	-0.1108	-0.1959
Δ HF	19.370	19.940	19.565	19.717	5.237	48.338	20.603	15.851

In Figure 7a, the SOMO is presented for the *o*-Cl derivative (**3**). It becomes evident that the lone electron of the molecular ion is delocalized mainly between C4a, C8a, N1, and O5 (maximal spin density always at C4a). A rather small part of spin density not accounting for the marked fragmentation differences can be attributed to *o*-Cl and *o*-Br substituents, but not to *o*-F, *o*-CH_3, and *o*-OCH_3. Neither the shape and the coefficients of the next two lower MOs nor the energy differences of microstates and eigenstates resulting from configuration interaction calculations correlate with the fragmentation behaviour. Also the charge distribution at the putative reaction centers is similar (the positive charge is delocalized and resides mainly at hydrogen atoms).

In conclusion, the energy minimum conformers do not show any property explaining why *o*-Cl and *o*-Br substituents, but not *o*-OCH_3 and *o*-CH_3 are easily split off. On the other hand, significant differences are observed for the "transition states" with substituents approaching O5. Whereas the *o*-F, the *o*-CH_3, and the *o*-OCH_3 derivative do not change their electronic structure compared to the minimum conformers, a marked alteration occurs in the cases of *o*-Cl and *o*-Br. Both substituents approach the O5 oxygen up to about 2.0 Å and become the main site of spin density. A further significant amount of spin density is localized at O5, whereas C4a and C8a do only slightly contribute to the overall spin. This points to an intramolecular "redox process": *o*-Cl and *o*-Br are "oxidized" in shifting an electron to the C4a-C8a π bond. More precisely: the new, energy-rich SOMO is formed by delivering an electron from the former SOMO-1 to the former SOMO. The positive charge is mainly located at the Cl or the Br atom, whereas O5 and C2' are markedly negative.

The SOMO of the "transition state" of the *o*-Cl derivative is presented in Figure 7b. It shows a reverse picture compared to the energy minimum. However, this snapshot does not directly point to the subsequent elimination-addition process including the real transition state. The elimination of *o*-Cl and *o*-Br radicals might be accompanied by attraction of an electron from a lower MO localized at O5. Then, the addition between O5 and C2' (distance of *ca.* 2.8 Å) would formally be the pairing of an oxygen and a phenyl radical. However, other mechanisms with forcing out the substituent by O5 are possible. A mechanism in the course of which O5 and C2' cyclizise *before* elimination of Cl or Br does not follow from the electronic structure. Additionally, if C2' rather than X had to approach to O5, rotation of the C4-C4a bond would be necessary, i.e., one of the two amide bonds must break. The respective ring-opened molecular ions are, however, more than 2 eV higher in energy than their cyclic analogues.

It must be noted that the quantitative differences of fragmentations between dichloro-substituted isomers cannot be explained by the calculations. Different distributions of lower MOs may come into play, but the semiempiric method is not precise enough to verify correlations with experimental findings. Also the reaction enthalpies of the fragmentation (Table 8) do not correlate with the experiment, since the ΔHF value of the OCH_3 molecular ion is more favourable compared to all *o*-Cl derivatives.

In conclusion, the results of the MO calculations support a direct displacement of *o*-Cl and *o*-Br substituents giving rise to a cyclized product ion **a** (Figure 3) which subsequently can lose $H^{\bullet}$ and HNCO. Reactive intermediates in accord with an addition-elimination mechanism are not likely.

EXPERIMENTAL PART

General remarks: Melting points: Büchi 5410, uncorrected; IR spectra: Nicolet 510M FT-IR; ^{1}H-NMR spectra: Varian EM 390 (90 MHz), Bruker WM 250 (250 MHz), TMS as int. standard, 90 MHz spectra if not otherwise stated; MS: Finnigan MAT 95 (70/12 eV), using a direct insertion probe (accelerator voltage 5 KV, ion source temp. *ca.* 200 °C). MIMS (1st ffr, B/E scan) and CA spectra: same instrument, same conditions. CA spectra were acquired by introducing He into the collision chamber (1st ffr, B/E linked scan) at such a rate that the intensity of the selected parent ion was reduced to *ca.* 20% of its

original value; TLC: SiO_2, Merck no 5554; Al-foils, Silica 60 F 254; CC: SiO_2 Merck no 7734 (silica 60; 70 - 230 mesh ASTM); solvents were purified and dried as usual; drying over Na_2SO_4; evaporation *in vacuo* at the rotary evaporator.

4-Substituted phenyl-4,6,7,8-tetrahydro-1H,3H-quinazoline-2,5-diones
General procedure:
The solution of 25.0 mmol of urea (N-methylurea for compound (**19**)), 25.0 mmol of the pertinent benzaldehyde, and 37.5 mmol of cyclohexane-1,3-dione in 100 mL of absol. EtOH and 5 - 6 drops of HCl (36%) was refluxed for 20 h. After cooling to rt the crystals were filtered off and recrystallized from EtOH / MeOH 1:1 (compound (**19**) was recrystallized from EtOH only without cooling in the refrigerator): colourless or faint yellow crystals.

4-Phenyl-4,6,7,8-tetrahydro-1H,3H-quinazoline-2,5-dione (**1**)[3a]

4-Deutero-4-phenyl-4,6,7,8-tetrahydro-1H,3H-quinazoline-2,5-dione (**1a**)
22 %, mp >220 °C. - IR: 3250, 3100 (N-H), 2970, 2900, 2880 (C-H), 1700 cm^{-1} (C=O). - ^{1}H-NMR (DMSO-d_6): δ (ppm) = 9.45 (s; 1H, NH), 7.75 (s; 1H, NH), 7.35 - 7.15 (m; 5H, aromat.), 2.50 - 1.75 (m; 6H, aliphat.).

4-Pentadeuterophenyl-4,6,7,8-tetrahydro-1H,3H-quinazoline-2,5-dione (**1b**)
52 %, mp >220 °C. - IR: 3210, 3100 (N-H), 2970, 2900, 2880 (C-H), 2270, 2250 (C-D), 1710 cm^{-1} (C=O). - ^{1}H-NMR (DMSO-d_6): δ (ppm) = 9.50 (s; 1H, NH), 7.75 (s; 1H, NH), 5.17 (d; 1H, J = 3.1 Hz, 4-H), 2.55 - 1.70 (m; 6H, aliphat.).

4-Deutero-4-pentadeuterophenyl-4,6,7,8-tetrahydro-1H,3H-quinazoline-2,5-dione (**1c**)
46 %, mp >220 °C. - IR: 3310, 3100 (N-H), 2950, 2900, 2870 (C-H), 2280 (C-D), 1710 cm^{-1} (C=O). - ^{1}H-NMR (DMSO-d_6): δ (ppm) = 9.50 (s; 1H, NH), 7.75 (s; 1H, NH), 2.50 - 1.70 (m; 6H, aliphat.).

4-(2-Chlorophenyl)-4,6,7,8-tetrahydro-1H,3H-quinazoline-2,5-dione (**3**)[15]

The *4,6,7,8-tetrahydro-1H,3H-quinazoline-2,5-diones* (**2, 4 - 14**) were prepared according to ref.[3a]

4-(2,6-Dichlorophenyl)-4,6,7,8-tetrahydro-1H,3H-quinazoline-2,5-dione (**15**)
20 %, mp >220 °C. - Anal. Calcd for $C_{14}H_{12}N_2O_2Cl_2$: C, 54.04; H, 3.89; N, 9.00. Found: C, 53.93; H, 4.05; N, 8.89. - IR: 3315, 3230, 3180 (N-H), 2980, 2950, 2900 (C-H), 1710 cm^{-1} (C=O). - ^{1}H-NMR (DMSO-d_6): δ (ppm) = 9.55 (s; 1H, NH), 7.60 (s; 1H, NH), 7.40 - 7.20 (m; 3H, aromat.), 6.10 (s; 1H, 4-H), 2.55 - 1.70 (m; 6H, aliphat.).

4-(2,3-Dichlorophenyl)-4,6,7,8-tetrahydro-1H,3H-quinazoline-2,5-dione (**16**)
56 %, mp >220 °C. - Anal. Calcd for $C_{14}H_{12}N_2O_2Cl_2$: C, 54.04; H, 3.89; N, 9.00. Found: C, 53.83; H, 4.00; N, 8.82. - IR: 3310, 3230, 3180 (N-H), 2980, 2920, 2870 (C-H), 1710 cm^{-1} (C=O). - ^{1}H-NMR (DMSO-d_6): δ (ppm) = 9.60 (s; 1H, NH), 7.73 (t; 1H, J = 2.2 Hz, NH), 7.55 - 7.15 (m; 3H, aromat.), 5.62 (d; 1H, J = 2.6 Hz, 4-H), 2.55 - 1.70 (m; 6H, aliphat.).

4-(2,4-Dichlorophenyl)-4,6,7,8-tetrahydro-1H,3H-quinazoline-2,5-dione (**17**)
50 %, mp >220 °C. - Anal. Calcd for $C_{14}H_{12}N_2O_2Cl_2$: C, 54.04; H, 3.89; N, 9.00. Found: C, 54.10; H, 4.01; N, 8.99. - IR: 3310, 3240, 3180 (N-H), 3050, 2960, 2930, 2870 (C-H), 1710 cm^{-1} (C=O). - ^{1}H-NMR (DMSO-d_6): δ (ppm) = 9.60 (s; 1H, NH), 7.70 (t; 1H, J = 2.2 Hz, NH), 7.55 - 7.15 (m; 3H, aromat.), 5.53 (d; 1H, J = 2.6 Hz, 4-H), 2.55 - 1.70 (m; 6H, aliphat.).

4-(3,4-Dichlorophenyl)-4,6,7,8-tetrahydro-1H,3H-quinazoline-2,5-dione (**18**)
61 %, mp >220 °C. - Anal. Calcd for $C_{14}H_{12}N_2O_2Cl_2$: C, 54.04; H, 3.89; N, 9.00. Found: C, 54.00; H, 4.02; N, 8.95. - IR: 3340, 3280 (N-H), 2970, 2930, 2890 (C-H), 1710, 1680 cm^{-1} (C=O). - ^{1}H-NMR

(DMSO-d_6): δ (ppm) = 9.60 (s; 1H, NH), 7.83 (t; 1H, J = 2.2 Hz, NH), 7.63 - 7.15 (m; 3H, aromat.), 5.20 (d; 1H, J = 2.9 Hz, 4-H), 2.55 - 1.70 (m; 6H, aliphat.).

1-Methyl-4-(2-chlorophenyl)-4,6,7,8-tetrahydro-1H,3H-quinazoline-2,5-dione (**19**)
36 %, mp 223-225 °C. - Anal. Calcd for $C_{15}H_{15}N_2O_2Cl$: C, 61.97; H, 5.20; N, 9.63. Found: C, 61.85; H, 5.30; N, 9.55. - IR: 3220, 3100 (N-H), 2970, 2950, 2880 (C-H), 1690 cm^{-1} (C=O). - ^{1}H-NMR (DMSO-d_6): δ (ppm) = 7.90 (d; 1H, J = 1.3 Hz, NH), 7.45 - 7.20 (m; 4H, aromat.), 5.56 (d; 1H, J = 1.2 Hz, 4-H), 3.17 (s; 3H, CH_3), 2.95 - 2.55 (m; 2H, aliphat.), 2.25 - 1.80 (m; 4H, aliphat.).

Major ions in the EIMS (70 / 12 eV; % rel. int.) of compounds (**1 - 19**)

1: 242 (88/100); 241 (34/1); 225 (2/-); 224 (1/-); 213 (4/-); 199(1/-); 198 (3/1); 186 (10/1); 185 (7/-); 165 (100/5); 77 (1/-); 55 (5/1).
1a: 243 (78/100); 242 (19/1); 241 (3/0.5); 214 (2/-); 200 (1/-); 199 (2/-); 187 (8/-); 186 (5/-); 166 (100/4); 165 (18/1); 77 (2/-); 55 (5/1).
1b: 247 (97/100); 246 (17/1); 245 (16/0.5); 218 (1/-); 217 (2/1); 202 (2/-); 191 (9/-); 189 (4/-); 166 (22/0.2); 165 (100/0.3); 82 (2/-); 55 (5/-).
1c: 248 (57/100); 247 (9/8); 246 (15/2); 230 (2/-); 228 (1/-); 227 (2/-); 218 (3/-); 203 (2/-); 192 (8/1); 191 (3/-); 190 (5/-); 166 (100/12); 82 (4/-); 166 (2/-); 82 (4/-); 55 (4/-).
2: 260 (64/100); 259 (16/1); 243 (2/-); 242 (1/-); 241 (8/2); 240 (29/12); 239 (100/33); 231 (4/-); 217 (2/-); 216 (4/-); 212 (2/-); 204 (19/1); 203 (7/-); 165 (98/6); 164 (6/6); 85 (9/-); 55 (8/-).
3: 278 (<0.1/<0.1); 277 (0.2/-); 276 (<0.1/<0.1); 275 (0.6/-); 241 (100/100); 240 (4/0.5); 239 (4/5); 222 (1/0.3); 220 (3/1); 198 (37/12); 165 (33/3); 55 (3/-).
4: 278 (13/29); 277 (9/14); 276 (42/100); 275 (11/1); 260 (1/-); 259 (2/-); 258 (1/-); 257 (3/-); 249 (1/-); 247 (3/-); 241 (44/20); 240 (1/-); 239 (2/-); 222 (2/-); 220 (6/1); 165 (100/18); 55 (9/1).
5: 278 (20/32); 277 (16/15); 276 (62/100); 275 (20/2); 260 (1/-); 259 (2/-); 258 (1/-); 257 (3/-); 249 (1/-); 247 (3/-); 241 (49/16); 240 (2/-); 239 (1/-); 222 (3/-); 220 (9/1); 165 (100/15); 55 (8/1).
6: 322 (<0.1/<0.1); 321 (0.3/-); 320 (<0.1/0.1); 319 (0.3/-); 266 (3/-); 264 (3/-); 241 (100/100); 240 (2/1); 239 (4/-); 198 (66/8); 197 (1/-); 196 (2/-); 165 (38/1); 55 (4/-).
7: 322 (31/98); 321 (12/14); 320 (31/100); 319 (7/1); 266 (4/-); 264 (4/-); 241 (60/17); 240 (1/-); 239 (2/-); 198 (3/-); 197 (1/-); 196 (1/-); 165 (100/14); 55 (7/-).
8: 322 (32/100); 321 (13/16); 320 (33/100); 319 (9/1); 266 (5/1); 264 (5/1); 241 (57/17); 240 (1/-); 239 (2/-); 198 (3/-); 197 (1/-); 196 (3/-); 165 (100/12); 55 (9/-).
9: 272 (65/100); 271 (20/2); 257 (6/1); 2451 (100/25); 240 (9/-); 239 (24/2); 216 (18/2); 198 (5/-); 197 (1/-); 196 (1/-); 165 (63/2); 55 (6/-).
10: 272 (59/100); 271 (20/2); 257 (4/1); 243 (7/-); 241 (38/7); 240 (3/1); 239 (8/1); 216 (13/1); 165 (100/6); 55 (7/-).
11: 272 (100/100); 271 (50/3); 257 (7/1); 243 (14/1); 241 (79/10); 240 (6/1); 239 (15/1); 216 (28/2); 165 (85/2); 55 (9/-).
12: 256 (26/100); 255 (16/12); 241 (34/10); 240 (1/2); 239 (10/14); 238 (33/39); 237 (7/2); 227 (2/-); 213 (10/8); 212 (2/-); 211 (2/1); 210 (8/4); 200 (7/1); 199 (3/-); 185 (3/-); 165 (100/15); 91(8/-); 55 (12/-).
13: 256 (63/100); 255 (21/2); 241 (32/5); 240 (1/-); 239 (2/-); 238 (3/-); 237 (3/-); 227 (4/-); 213 (2/-); 212 (3/-); 211 (1/-); 210 (1/-); 200 (9/1); 199 (5/-); 185 (4/-); 165 (100/7); 91 (7/-); 55 (7/-).
14: 256 (84/100); 255 (33/3); 241 (54/6); 240 (1/-); 239 (4/-); 238 (4/-); 237 (4/-); 227 (6/-); 213 (3/-); 212 (4/-); 200 (15/1); 199 (9/-); 185 (6/1); 165 (100/5); 91 (8/-); 55 (8/-).
15: 314 (0.1/0.4); 312 (1.5/2.4); 310 (2.3/3.7); 277 (31/24); 276 (16/17); 275 (100/100); 274 (3/2); 273 (5/-); 258 (2/-); 256 (9/-); 254 (14/1); 240 (10/1); 239 (62/3); 234 (23/2); 232 (73/8); 196 (8/-); 184 (9/1); 165 (62/2); 55 (7/-).

16: 314 (<0.1/<0.1); 312 (<0.1/<0.1); 310 (0.1/<0.1); 277 ((34/33); 275 (100/100); 274 (4/-); 273 (4/-); 258 (1/-); 256 (3/-); 254 (5/-); 234 (14/2); 232 (42/7); 184 (1/-); 165 (53/2); 55 (6/-).

17: 314 (<0.1/<0.1); 313 (0.2/-); 312 (0.5/0.6); 311 (0.6/0.1); 310 (0.9/1); 277 (32/33); 275 (100/100); 274 (3/3); 273 (4/-); 258 (1/-); 256 (3/-); 254 (5/-); 234 (16/2); 232 (48/6); 184 (3/-); 165 (44/2); 55 (7/-).

18: 314 (3/9); 313 (3/9); 312 (19/65); 311 (9/15); 310 (29/100); 309 (8/2); 277 (21/11); 275 (64/36); 274 (1/0.5); 273 (2/-); 258 (1/-); 256 (4/0.5); 254 (6/1); 234 (3/-); 232 (10/1); 165 (100/14); 55 (11/-).

19: 292 (0.3/0.6); 291 (0.3/0.2); 290 (0.9/1.8); 289 (0.6/0.1); 255 (100/100); 254 (4/3); 253 (5/-); 236 (0.7/-); 234 (2/-); 212 (32/2); 179 (51/2); 55 (5/-).

ACKNOWLEDGMENT

We thank Fonds der Chemischen Industrie, Frankfurt / Main, Germany, for financial support of this project.

REFERENCES

1 a) J. J. Van den Eynde, N. Audiart, V. Camone, S. Michel, Y. Van Haverbeke, and C. O. Kappe, *Heterocycles,* 1997, **45**, 1967; b) C. O. Kappe, *Tetrahedron*, 1993, **49,** 6937 and lit. cited therein.

2 R. Fossheim, *J. Med. Chem.*, 1986, **29,** 305.

3 a) S. Sarac, M. Yarim, M. Ertan, S. Boydag, and K. Erol, *Pharmazie*, 1998, **53**, 91; b) S. Sarac, M. Yarim, M. Ertan, K. Erol, and Y.Aktan, *Boll. Chim. Farm.*, *1998*, in press.

4 a) E. E. Stashenko, P. J. Zakharov, V. G. Pleshakov, and B. S. Subbotin, *Khim. Geterosikl. Soed.*, 1989, 360 (*Chem. Abstr.*, 1989, **111**, 214037); b) L. Yu. Ivanoskaya, Z. D. Dubovenko, and V. P. Mamaev, *Izv. Sib. Otd. Akad. Nauk SSSR, Ser. Khim. Nauk*, 1969, 132 (*Chem. Abstr.*, 1970, **72**, 66892 k).

5 G. Sindona, R. Weber, and K. Levsen, *Adv. Mass Spectrom.*, 1980, **8**, 879.

6 J. J. Gallagher, E. K. Chess, S. M. Arghestani, and M. L. Gross, *Org. Mass Spectrom.*, 1983, **18**, 118.

7 M. A. Baldwin, F. W. McLafferty, and D. M. Jerina, *J. Am. Chem. Soc.*, 1975, **97**, 6169.

8 J. Fossey, D. Lefort, and J. Sorba, *Free Radicals in Organic Chemistry*, Wiley, 1995.

9 H. Schwarz, *Topics in Current Chem.*, 1978, **73**, 231.

10 B. Schaldach, B. Grotemeyer, J. Grotemeyer, and H.-Fr. Grützmacher, *Org. Mass Spectrom.*, 1981, **16**, 410.

11 B. Schaldach and H.-Fr. Grützmacher, *Org. Mass Spectrom.*, 1980, **15,** 175.

12 P. J. Smith, J. R. Dimmock, and W. A. Turner, *Canad. J. Chem.*, 1973, **51**, 1458.

13 H.-Fr. Grützmacher, *Org. Mass Spectrom.*, 1993, **28**, 1375.

14 K. Levsen and H. Schwarz, *Mass Spectrom. Rev.*, 1983, **2**, 77.

15 Y. F. Chi and Y. L. Wu, *Huaxue Xuebao*, 1956, **22**, 188 (*Chem. Abstr.*, 1958, **52**, 6360g).

Received, 5th February, 1998